Propagation of the centroid of the Poynting vector in transversely phase-modulated optical beams in spatially dispersive media

Aminul I. Talukder,[1,*] Tsuyoshi Matsuo,[1,*] Takahiro Matsumoto,[2] and Makoto Tomita[1]

[1]*Department of Physics, Faculty of Science, Shizuoka University, 836 Ohya, Suruga-ku, Shizuoka 422-8529, Japan*

[2]*Research and Development Center, Stanley Electric Corporation, 5-9-5 Tokodai, Tsukuba 300-2635, Japan*

The propagation of an optical beam in dispersive medium is described by a spatial analog of pulse propagation in time domain. In particular, the evolution of transverse beam profiles with transversely complicated wave fronts passing through spatially dispersive media is examined and explained on the basis of net group and reshaping shifts in the ω and $\vec{k}$ domains. The experimental results are in good agreement with the theory of net group and reshaping delays as described by Peatross *et al.* [J. Peatross, S. A. Glasgow, and M. Ware, Phys. Rev. Lett. **84**, 2370 (2000)], which successfully described the arrival time for optical pulses through frequency dispersive media.

PACS number(s): 42.25.Bs, 41.20.Jb

I. INTRODUCTION

The concept of group velocity, as applied to wave motion, is particularly useful for describing the propagation velocity. The fundamental concept of group velocity was first introduced by Hamilton [1] in 1839, before the works of Stokes [2], Rayleigh [3], Sommerfeld and Brillouin [4–6]. The phenomena of slow and fast light, in which pulse propagation is manipulated mainly by frequency dispersion based on the quantum control of coherence in cooled atoms or in solids and nanophotonic structures, have attracted a great deal of attention. Slow light refers to the case $v_g \ll c$ and occurs in the case of a system with large normal dispersion. Effects such as slow pulse propagation and the freezing or storage of light have been observed in cooled atomic vapors [7–10]. Fast light has a longer history. It is defined as $v_g > c$ or $v_g < 0$, and can be observed in the case of very large anomalous dispersion [11,12]. Garret and McCumber [13] were the first to point out that a Gaussian-shaped wave packet propagates at the conventional group velocity, v_g, even when $v_g > c$ or $v_g < 0$. Chu and Wong [14] performed experiments with fast light propagation through an absorption resonance to investigate the predictions of Garret and McCumber. They showed that the group velocity is a useful concept for describing a significant advance, even in the case of compression in the shapes of outgoing wave packets. The key experimental tool in their studies [13,14] was a narrow spectral width for their wave packet and a propagation distance short enough that the higher-order dispersive effects could be neglected.

For pulse propagation in dispersive media, conventional analysis within the group velocity approximation is given on the basis of the expansion, $k(\omega) = k(\omega_0) + [\partial k(\omega)/\partial \omega](\omega - \omega_0) + [\partial^2 k(\omega)/\partial^2 \omega](\omega - \omega_0)^2 + \cdots$. The first term adds a constant to the phase. The second term adds a delay to the wave packet and is understood as a conventional group velocity defined as $v_g = v_z[t] = (\frac{\partial \omega}{\partial k_z})^{-1} = \frac{c}{\omega[dn(\omega)/d\omega]+n}$, describing the motion of a wave packet in a dispersive medium over a short propagation distance, i.e., under conditions where the

packet retains its shape and dimensions. The third term in the expansion is the group delay dispersion, also known as the group velocity dispersion. During propagation, a wave packet of a certain spectral width will broaden due to group velocity dispersion. The fourth term is the third-order dispersion, which applies a cubic phase across the wave packet.

A recurring problem over the last century was the development of a concept of group velocity that was valid over long propagation distances, i.e., under conditions where the outgoing packet was severely deformed and lost its individuality. Tanaka *et al.* [15] used the saddle-point method, taking the imaginary part of the refractive index into account, and showed that the spectral shift in the wave packet should be taken into consideration, especially for broad spectral-width packets. They concluded that the group velocity at the carrier frequency had no meaning. However, the peak of the outgoing wave packet dominated by the surviving spectrum was significant, even over long propagation distances. Although it has been experimentally confirmed [12], Tanaka *et al.* considered only a Gaussian wave packet and their definition was not robust, particularly for wave packets with complicated structures, e.g., with asymmetric rising or falling or with multiple peaks. Peatross *et al.* [16] proposed that the group velocity had physical significance under all conditions when considering the average energy flow that is the center of gravity (centroid) of the Poynting vector—instead of the peak—of the wave packet as the arrival time. This was actually first proposed by Schwinger *et al.* [17]. Nevertheless, a neat separation of total delay into the net group delay and reshaping delay by Peatross *et al.* made this method attractive for describing the wave propagation. In their definition, a time expectation integral over the Poynting vector is used. In fact, the importance of net group and reshaping delays in frequency dispersive media was confirmed subsequently by the experimental measurements [18].

In all of the above discussions, the wave propagation described by group velocity was discussed in terms of frequency or time dispersion, where the medium function ϵ depended on ω, i.e., $\varepsilon = \varepsilon(\omega)$. It may be interesting to extend the problem into the spatial dispersion domain, where the medium function also depends on the wave vector $\vec{k}$, i.e., $\varepsilon = \varepsilon(\omega, \vec{k})$.

___

*These authors contributed equally to the work.
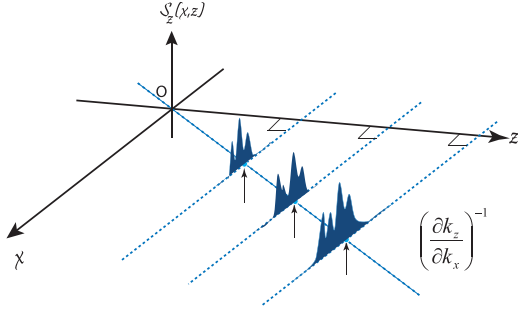
FIG. 1. (Color online) Schematic cross-section profiles of the beam along the x axis, while the beam is propagating in the z direction. The upward arrows indicate the x positions of the profile centroids.

In 1978, Polevoi and Rytov discussed the propagation of electromagnetic wave packets in electrically and magnetically anisotropic media possessing space-time dispersion [19]. Starting with the four-dimensional form of the fundamental Maxwell equations, they were able to introduce a simple expression for the group 4-velocity. In fact, spatial dispersion effects are usually much weaker than those arising from frequency dispersion, but the effects can result in some new phenomena in physics. In addition to the study of effects such as stopping light in hot atoms based on the spatial dispersion of refractive index [20] or the possibility of engineering new artificial materials (meta-materials), an interesting possibility appears when considering the aspects of negative group velocity, that is, the manipulation of strong spatial dispersion profiles [21,22]. Superprism effects, or the directional control of light in which the light beam enters through one facet of a prism and exits from another facet, has also been an attractive phenomenon [23–25]. Superprism effects permit the creation of ultrahigh-resolution spectroscopes, which is impossible using traditional gratings. Therefore, it may be of interest to consider a very steep spatial dispersion and to examine the wave propagation through it, especially from the viewpoint of beam steering. In this study, we apply the concept of net group and reshaping delays to an analogous spatial domain, and discuss whether the propagation of an arbitrarily shaped transverse beam profile can be described in terms of the net group and reshaping shifts, in the spatial (ω and $\vec{k}$) domain, in the absence and presence of attenuation, respectively.

II. THEORY

To develop the concept of group velocity in the ω and $\vec{k}$ domains, we start with a simple case of a monochromatic light wave propagating through a homogeneous isotropic nonmagnetic medium that satisfies the Helmholtz equation,

$$\nabla^2 \vec{E}(x,y,z,t) = -\left(\frac{n\omega}{c}\right)^2 \vec{E}(x,y,z,t). \qquad (1)$$

Here, n is the refractive index. Suppose a monochromatic laser beam with an arbitrary profile in the x direction (x profile), propagates a distance within the $x - z$ plane, as shown in Fig. 1. The input field in Eq. (1) can be written as $\vec{E}(x,y,z,t) \rightarrow$

$\vec{E}(x,z)e^{-i\omega_0 t}$. If

$$\vec{E}(k_x,0) = \frac{1}{\sqrt{2\pi}} \int \vec{E}(x,0)e^{-ik_x x}dx \qquad (2)$$

is the Fourier component composing the initial x profile of the beam, the output beam profile can be written as

$$\vec{E}(x,z) = \frac{1}{\sqrt{2\pi}} \int \vec{E}(k_x,0)e^{i(k_x x - k_z z)}dk_x, \qquad (3)$$

where $k_z(k_x)$ can be expanded around k_{x_0} as

$$k_z(k_x) = k_{z_0} + \frac{\partial k_z(k_x)}{\partial k_x}|_{k_{x_0}}\left(k_x - k_{x_0}\right)$$

$$+ \frac{1}{2}\frac{\partial^2 k_z(k_x)}{\partial k_x^2}|_{k_{x_0}}\left(k_x - k_{x_0}\right)^2 + \cdots, \qquad (4)$$

and $\omega_0/k_0 = c$. Neglecting the higher-order terms in Eq. (4), Eq. (3) reduces to

$$\vec{E}(x,z) = \vec{E}\left[x - \frac{\partial k_z(k_x)}{\partial k_x}\bigg|_{k_{x_0}}z,0\right]e^{i\phi}, \qquad (5)$$

where $\phi = (k_{z_0} - k_{x_0}\{\frac{\partial k_z(k_x)}{\partial k_x}\}|_{k_{x_0}})z$, and the velocity at which the slowly varying envelope moves, $v_{gx} \equiv G_{zx} = (\{\frac{\partial k_z(k_x)}{\partial k_x}\}|_{k_{x_0}})^{-1}$, are used in the simplification. v_{gx} is the transverse group velocity and is proportional to the shift in the x position of the profile. Here, z is perpendicular to the x plane and, in the case of free space, $\vec{k}$ has x and z components that are related by

$$k_z(k_x) = \left(k_0^2 - k_x^2\right)^{1/2} = k_0 + \frac{1}{2k_0}k_x^2 - \frac{1}{8k_0^3}k_x^4 + \cdots. \qquad (6)$$

A. Net and reshaping shift

We now consider the $\partial k_x/\partial k_z$ term and discuss the arrival of the x profiles of the beam as a function of propagation distance z for a medium dispersive in the $\vec{k}$ domain. It is similar to the term $\partial \omega/\partial k$, which is used to describe the temporal position of a wave packet, propagating along the z axis, through a medium dispersive in ω. In the present work, our interest is in situations where the cross section of the beam has an arbitrary presupposed profile that evolves into a complicated structure in both the amplitude and phase when propagating through a strong spatially dispersive medium. For example, as shown in the schematic in Fig. 1, the peak position of the beam profile cannot be tracked well if it contains multiple peaks, nonuniform rising, or both, and if it deforms significantly because of the effect of the higher-order terms in Eq. (4). Using the definition of arrival time in [16], the x position of the beam can be defined by the profile centroid,

$$\langle x \rangle_z = \frac{\hat{u}_z \cdot \int_{-\infty}^{\infty} x\vec{S}(x,z)dx}{\hat{u}_z \cdot \int_{-\infty}^{\infty} \vec{S}(x,z)dx}, \qquad (7)$$

where $\vec{S}(x,z) = \vec{E}(x,z) \times \vec{H}^*(x,z)$ is the Poynting vector. Using the definition of Eq. (7), we can develop a discussion similar to the net group and reshaping delays for pulse propagation through a strong frequency dispersive medium

[16]. In this approach, the transverse shift of the beam (x positions) between the longitudinal propagation distances z_0 and z is given by

$$\Delta x \equiv \langle x \rangle_z - \langle x \rangle_{z_0} = \Delta x_G + \Delta x_R. \qquad (8)$$

The first term on the right-hand side of Eq. (8), the net group shift, is a spatial average of the conventional group delay weighted by the output $\vec{k}$ vectors,

$$\Delta x_G = \left\langle \frac{\partial \mathrm{Re} k_z}{\partial k_x} \Delta z \right\rangle_z$$

$$= \frac{\int_{-\infty}^{\infty} \left[\frac{\partial \mathrm{Re} k_z}{\partial k_x} \Delta z \right] S_z(k_x, z) dk_x}{\int_{-\infty}^{\infty} S_z(k_x, z) dk_x}, \qquad (9)$$

where $S_z(k_x, z)$ is the z component of the Poynting vector $\vec{S}(k_x, z)$. The second term in Eq. (8) is called the reshaping shift in the x position, denoted by

$$\Delta x_R \equiv T[e^{-\mathrm{Im} k_z(k_x) \Delta z} \vec{E}(k_x, z_0)] - T[\vec{E}(k_x, z_0)], \qquad (10)$$

where

$$T[\vec{E}(k_x, z)] \equiv -i \frac{\hat{u}_z \cdot \int_{-\infty}^{\infty} \frac{\partial \vec{E}(k_x, z)}{\partial k_x} \times \vec{H}^*(k_x, z) dk_x}{\hat{u}_z \cdot \int_{-\infty}^{\infty} \vec{S}(k_x, z) dk_x}. \qquad (11)$$

Net group and reshaping shifts for spatial dispersion are similar to net group and reshaping delays for pulse propagation in a frequency dispersive medium. The net shift is the expectation integral over the surrounding spectrum. Therefore, if the Poynting vector, $\vec{S}(k_x, z)$, does not change in k_x space, the net shift remains the same for coherent (Gaussian) and irregularly shaped beams. When the bandwidth, Δk_x, of the incident beam is narrow as $S_z(k_x) \to \delta(k_x)$, the factor $\partial \mathrm{Re}[k_z]/\partial k_x$ may fall outside the integral, in which case the simple group velocity, $\partial \mathrm{Re}[k]/\partial \omega$ is obtained. The reshaping shift appears from the initial organization of the phase of the beam and its spectral change during propagation. Thus, the reshaping shift will be zero if there is no phase modulation or any spectral change through the medium.

III. EXPERIMENTS AND RESULTS

In our previous study [18], we verified the concept of net group and reshaping delays in terms of arrival time for arbitrarily shaped wave packet propagation in frequency dispersive media. As the transverse component of group velocity attributed to the spatial dispersion is an area of recent interest, especially in terms of its application, it is important to obtain experimental verification of the net group and reshaping effects in the $\vec{k}$ domain. The concept of both net group and reshaping effects may be examined individually in a well-designed experimental system. Figure 2 illustrates the measurement configuration. A single-mode coherent He-Ne laser was used as the beam source. The well-collimated beam passed through a pair of Fourier transform lenses (L1 and L2) with focal lengths $f1 = f2 = 80$ cm. The beam diameter was $\sim$10 mm at the Fourier plane of the lenses. A liquid crystal on silicon–spatial light modulator (LCOS-SLM; Hamamatsu Photonics) consisting of a matrix of 792×600 rectangular pixels (16 mm $\times$ 12 mm) was placed at the Fourier plane to modulate the phase or to shape the beam into a complex form

with multiple peaks. In our experimental setup, the 792-pixel side (16-mm side) of the LCOS-SLM is oriented along the x axis (transverse direction) and modulates the phase of the vertically polarized light components. Although it is possible to introduce a two-dimensional arbitrary phase in the k_x and k_y domains, we implemented an arbitrary phase modulation $\phi(k_x)$ only in the x direction, i.e., $\vec{E}(k_x, k_y) = \vec{E}(k_x)$, by applying a masking function of $\vec{E}(k_x) \propto \exp[i\phi(k_x)]$ on LCOS-SLM with computer programming. The maximum k_x bandwidth can be determined by the minimum pixel size of the LCOS-SLM; i.e., $\Delta k_x = $ (LOCOS pixel size)$^{-1} = 49.5$ mm^{-1}, and the k_x-space resolution is determined by the incident laser beam size, $\delta k_{x\,\mathrm{min}} = $ (laser beam size)$^{-1} = 0.1$ mm^{-1}. Free-space propagation was used in our experiment. For the net group shift measurements, the output beam was monitored for different propagation distances, z, where the zero point ($z = 0$) was located at a position near the resettable mirror (RSM), 0.8 m from L2, as shown in Fig. 2(a). The charge-coupled device (CCD) detector used for monitoring the x profile of the beam was placed on a translation rail such that its position could be moved forward or backward for different z. For the reshaping shift measurements, we used reflection near a total internal reflection to introduce steep k-dependent attenuation of the beam. For this purpose, the RSM was removed and the beam took path (b) through a silica prism, as shown in Fig. 2. The prism was set on a rotational stage, which allowed us to induce beam attenuation with respect to the beam's total internal reflection (TR). The top inset of Fig. 2 shows the reflectance curve of the prism as a function of the incident angle (θ) of the beam on the prism boundary. In this case, the detector (CCD) was fixed at a point near $z = 0$ so that the net group shift would be negligible. Our setup was well designed for individual measurements of net group and reshaping shifts in the $\vec{k}$ domain.

Net group shift experiments were performed for both a Gaussian beam and irregularly shaped beam. The four major peaks of irregularly shaped beam are denoted by filled diamonds, filled circles, open circles, and upward triangles in Fig. 3. A Gaussian beam was used as a reference in our experiment, and its initial phase was set to $\phi(k_x) = 0$, while a phase modulation of $\phi(k_x) = \phi_{\mathrm{irregular}}$ was applied to achieve the initial irregularly shaped beam. The left column shows the output x profiles for both types of beams observed at different propagation distances, z. The centroid position of the irregularly shaped beam was investigated using the Gaussian beam centroid as a reference, indicated by the downward arrow in Fig. 3(a). The transverse profiles of irregularly shaped beams widened and deformed significantly with increasing propagation distance, evolving new peaks at the expense of the originals, as shown by the downward triangles in the profiles, Figs. 3(b)–3(e). However, in all cases, the center of gravity positions remained constant with respect to those of the Gaussian beams. We also examined the propagation of the Gaussian and irregularly shaped beams by applying linear phase modulation of $\phi(k_x) = Ak_x$ and $\phi(k_x) = \phi_{\mathrm{irregular}} + Ak_x$, respectively, on the incident beams; A is a constant in this study. The right column in Fig. 3 shows the resultant output x profiles, which are similar to those in the left column. Indeed, we see a shift in the centroid position
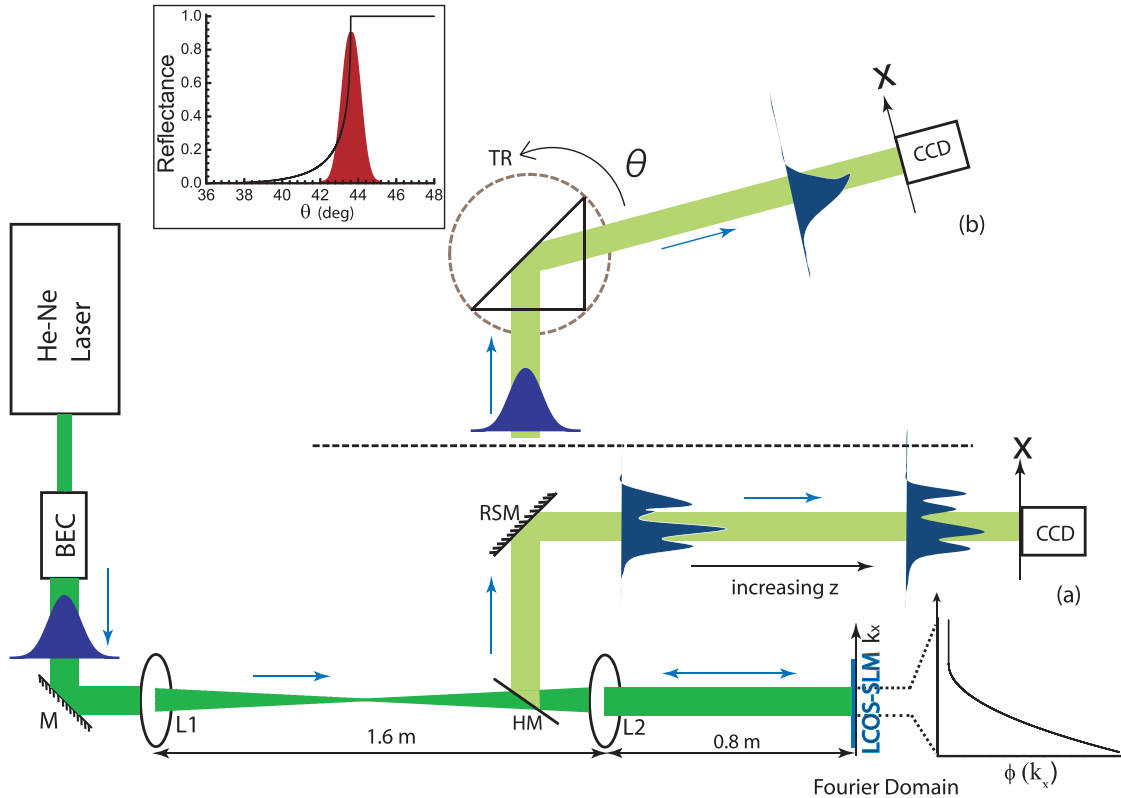
FIG. 2. (Color online) Schematic of the experimental setup. BEC is the beam expander with collimation, M is the mirror, L1 and L2 are lenses with equal focal lengths of 80 cm, HM is the half mirror, RSM is the resettable mirror, and CCD is the charge-coupled device (CCD) camera. LCOS-SLM is the liquid crystal on silicon–spatial light modulator. The modulation of k_x components is projected at the right side of LCOS-SLM. For net group shift measurements, the beam takes path (a). For reshaping shift measurements, the RSM is removed and the beam takes path (b) through a prism on a rotational stage. The top inset shows the reflection curve of the prism when rotated towards its total internal reflection (TR) point. The output profile symmetry is curtailed, as shown by the profile in front of the CCD in path (b).

from that shown in the left column for both types of beam because of the linear phase modulation of the input beam. The peak has no significance, as the initial beam contains multiple peaks. However, the centroid of the Poynting vector retains its physical significance and remains precisely the same for both the irregularly shaped beam and the Gaussian beam, demonstrating one of the predictions of net group delay.

The incident beam in our experiment has a complex structure, containing multiple peaks in $\vec{k}$ space. Therefore, the expectation integral in Eq. (7) can be used to define the beam shift in the x direction. The net group shift depends on the power spectrum of the beam and is independent of the phases of the field components, $\phi(k_x)$. As the power spectrum is the same for these two cases in our experiments, the net group shift (the relative movement of the beam centroids) will be the same for the irregularly shaped and Gaussian beams for any propagation distance, z. This is demonstrated in the graphs presented in Fig. 4. It is obvious that the linear phase modulation shifts the centroid of the beam compared to the centroid of the beam without linear phase modulation. However, in accordance with the concept of net group shift, the relative movements of the centroids as a function of propagation distance are the same for both the Gaussian and the irregularly shaped beams, as shown in the upper portion of Fig. 4. The solid lines are the theoretically calculated shifts in the centroids, computed using

Eq. (9). All measurements show excellent agreement with the predictions of net group delay.

To measure the reshaping shift, we produced a linearly chirped beam by applying phase modulation on the Gaussian beam from LCOS-SLM. The phase modulation of the k_x components in such a case can be described by the equation $\phi(k_x) = B(k_x - C)^2$, which is shown as a schematic curve beside LCOS-SLM in Fig. 2; B and C are constants in this study. As mentioned earlier, a steep angle-dependent reflectivity near the total internal reflection (TR) of a conventional silica prism was used in this case. The $\vec{k}$ bandwidth of the total internal reflection (i.e., the range over which the reflection of the prism rises from 30% to 90%) was estimated to be $\gamma = 50$ mm^{-1}. When the bandwidth, Δk_x, of the incident beam is narrow compared to the prism bandwidth, γ, $v_{gx} = \frac{\partial \text{Re}[k_z]}{\partial k_x}$ then applies. However, in the present case, $\Delta k_x \approx \gamma$, a sharp attenuation causes strong reshaping in the transmitted beam, and the centroid of the transmitted beam can be explained by the reshaping shift defined in Eq. (10).

The reshaping effect is sensitive to the phase modulation. It occurs through absorption or amplification during propagation. A transverse linear phase chirped beam, under the effects of absorption or amplification, will experience a shift in the centroid position. The positions of the centroids do not change (or the reshaping shift is zero) for a narrow band
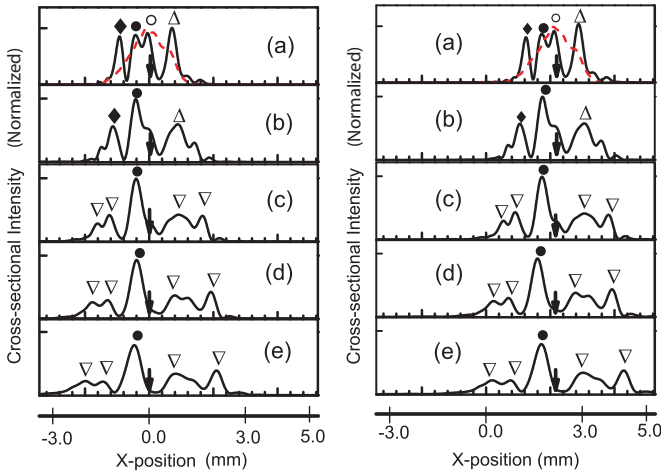
FIG. 3. (Color online) The cross-sectional profile of the beam along the x axis for different propagation distances, z: (a) 0.8 m, (b) 1.0 m, (c) 1.2 m, (d) 1.4 m, and (e) 1.6 m. The left column shows the observed x profiles for a Gaussian (red-dashed curve) and an irregularly shaped (solid curve) beam, while the right column shows the same when a linear modulation is applied to the beams represented in the left column. The horizontal axes for both graphs describe the absolute translation in the x direction where the centroid of a Gaussian beam is estimated to be at zero. The relative positions of the centroids of the Gaussian and irregularly shaped beams coincide precisely, as indicated by the downward arrows in the graphs. The solid diamonds, solid circles, open circles, and upward triangles mark the four major peaks of the irregularly shaped beam profile. The profile is seen to widen and deform severely with increasing propagation distance, evolving additional peaks, as shown by the downward triangles in (b)–(e) in the left and right columns.

limit, $\Delta k \ll \gamma$, even when the beam suffers attenuation or amplification. It is also true that the reshaping shift is zero if the input beam has no phase modulation, i.e., $\phi(k_x) = $ constant (Gaussian beam). In our reshaping shift experiment, we
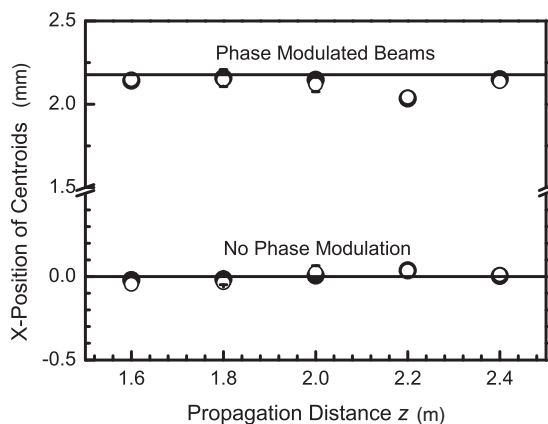
FIG. 4. The net group shift as a function of propagation distance, z. The solid and open circles at the lower side of the graph mark the relative shifts in the centroids for the Gaussian and irregularly shaped beams, respectively, without linear phase modulation from LCOS-SLM. The upper portion of the graph shows the shifts when a linear phase chirp is applied from LCOS-SLM to the beams described in the lower portion. The solid lines correspond to calculations made using Eq. (9).
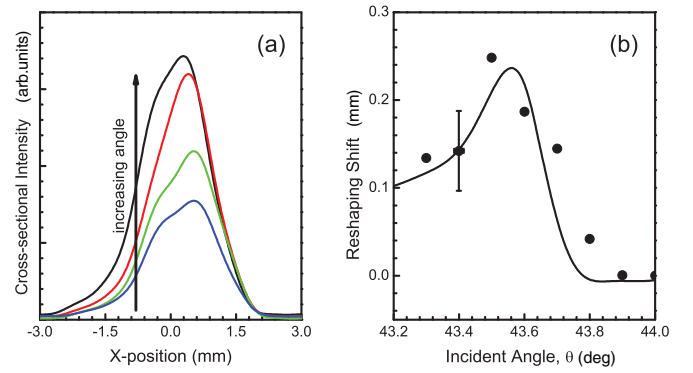
FIG. 5. (Color online) (a) Cross-sectional intensity profiles of the chirped beam, observed along the x direction, for four different incident angles θ of the prism, 43.3°, 43.5°, 43.6°, and 43.8°, where the simple beam shift due to the prism rotation is adjusted in the graph. The upward arrow indicates the direction of increasing θ for the curves. The profile intensity was normalized to the maximum of the intensity for an unchirped beam incident at an angle much larger than θ_c of the prism. (b) The shifts in the centroids of the x profiles as a function of incident angle, θ. The solid circles indicate the centroids of the experimentally observed x profiles, while the solid line represents the centroids obtained from a simulation created using Eq. (10). The $x = 0$ position was estimated at the centroid of an unchirped beam incident at an angle larger than θ_c of the prism.

introduced attenuation to the propagating beam by changing the incident angle with respect to the critical angle (θ_c) for the total internal reflection (TR) of the prism. Figure 5(a) shows the observed x profiles for different incident angles, θ, of the beam, where the simple beam shift due to the prism rotation, 2θ, is subtracted in the graph. The profiles are deformed from one side; hence, the centroid is shifted. When the prism is rotated clockwise, the k_x components on the positive x side are more strongly attenuated than those on the negative x side of the beam; hence, the profiles are distorted, which is attributable to the reshaping effect. Figure 5(b) summarizes the changes in reshaping shift with incident angle, θ. The reshaping shift increases with increasing θ (rotating the prism anticlockwise), which is attributable to phase modulation of the k_x components of the beam and the transfer function of the prism (refer to the top inset of Fig. 2). As θ approaches θ_c ($\sim$43.6°), the reshaping shift decreases with increasing θ because of the smaller beam deformation. It drops to zero at an angle $\theta \geqslant \theta_c$. The reshaping shift calculated using Eq. (10) is represented by the solid line in Fig. 5(b), and is in good agreement with the shift observed in our experiment.

IV. DISCUSSION

In studying wave propagation, only the group velocity v_g in the z direction has been considered. By generalizing to four dimensions, it is possible to also deal with the group velocity in other directions. Similar to the above calculation, it can be shown that the group velocity satisfying the wave equation in a four-dimensional (4-vector or tensor) generalization may be

expressed by the following relationship:

$$
G_{\mu v} =
\begin{pmatrix}
\dfrac{\partial k_0}{\partial k_0} & \dfrac{\partial k_1}{\partial k_0} & \dfrac{\partial k_2}{\partial k_0} & \dfrac{\partial k_3}{\partial k_0} \\[2ex]
\dfrac{\partial k_0}{\partial k_1} & \dfrac{\partial k_1}{\partial k_1} & \dfrac{\partial k_2}{\partial k_1} & \dfrac{\partial k_3}{\partial k_1} \\[2ex]
\dfrac{\partial k_0}{\partial k_2} & \dfrac{\partial k_1}{\partial k_2} & \dfrac{\partial k_2}{\partial k_2} & \dfrac{\partial k_3}{\partial k_2} \\[2ex]
\dfrac{\partial k_0}{\partial k_3} & \dfrac{\partial k_1}{\partial k_3} & \dfrac{\partial k_2}{\partial k_3} & \dfrac{\partial k_3}{\partial k_3}
\end{pmatrix}.
\tag{12}
$$

The details of this four-dimensional group velocity and its generalization in a medium with space-time dispersion will be discussed elsewhere. Usually, four-dimensional group velocity, which has a functional dependence of $G_{\mu v}(\vec{k},\omega)$, is difficult to study compared to the traditional group velocity, v_g. A large number of higher-order terms in the expansion in ω and $\vec{k}$ domains complicate the net group effect. The parameters of wavelength and angle of incidence introduce additional complications to the reshaping effect, which is due to the attenuation or amplification of various $\vec{k}$ components on a boundary. However, the decomposition of the propagation velocity into net group and reshaping shifts (delays) has enabled us to study both effects individually in strong spatially dispersive (present case) and frequency dispersive (Ref. [18]) media.

In a recent study of the propagation velocity of pulses [26], the arrival of the temporal ($\langle t \rangle = [\hat{u} \cdot \int t \vec{S}(x,t)dt]/[\hat{u} \cdot \int \vec{S}(x,t)dt]$) and spatial ($\langle x \rangle = [\hat{u} \cdot \int x \vec{S}(x,t)dx]/[\hat{u} \cdot \int \vec{S}(x,t)dx]$) centroids for wave packets were discussed on the basis of real-ω, $dk/d\omega$, and real-k, $d\omega/dk$, expansions, respectively. It was shown that the group

velocities defined by the arrival of temporal and spatial beam profiles along the z direction in a frequency dispersive medium are unlikely to be equal. In the above study, only longitudinal group velocity (i.e., $\frac{\partial k}{\partial \omega}$ or $\frac{\partial \omega}{\partial k}$) was considered. In contrast, in the present study, the transverse group velocity ($\frac{\partial k}{\partial k}$) was studied and explained in terms of net group and reshaping shifts along the x direction in the absence and presence of beam attenuation.

V. CONCLUSION

The propagation of light in spatially dispersive media was described by a spatial analog of pulse propagation in time domain. The propagation shifts in the spatial dimension for transversely shaped arbitrary beam profiles were measured to good experimental accuracy in the absence and presence of attenuation, and mathematically described in the context of net group and reshaping shifts, respectively. The centroids of x profiles for Gaussian and irregularly shaped phase-modulated beams remained the same in the case of free-space propagation, although the profiles suffered severe deformation with propagation distance. To date, there have been no reports discussing this transverse group velocity in free space or even presentation of any experimental verification. When a transversely phase-modulated beam propagates through a medium that will attenuate the beam in $\vec{k}$ space, the centroid of the Poynting vector changes; specifically, reshaping occurs due to the attenuation of the k_x components. The experimental results were in good agreement with the theory of net group and reshaping delays.

[1] W. R. Hamilton, Proc. R. Ir. Acad. **1**, 341 (1839).

[2] G. G. Stokes, Smith's Prize Examination Question, 2 February 1876, reprinted in G. G. Stokes, *Mathematical and Physical Papers* (Cambridge University Press, Cambridge, 1905), Vol. 5, p. 362.

[3] Lord Rayleigh, Proc. London Math. Soc. **9**, 21 (1877).

[4] L. Brillouin, Ann. Phys. (Leipzig) **44**, 203 (1914).

[5] A. Sommerfeld, Ann. Phys. (Leipzig) **44**, 177 (1914).

[6] L. Brillouin, *Wave Propagation and Group Velocity* (Academic Press, New York, 1960).

[7] L. V. Hau, S. E. Harris, Z. Dutton, and C. H. Behroozi, Nature **397**, 594 (1999).

[8] M. M. Kash, V. A. Sautenkov, A. S. Zibrov, L. Hollberg, G. R. Welch, M. D. Lukin, Y. Rostovtsev, E. S. Fry, and M. O. Scully, Phys. Rev. Lett. **82**, 5229 (1999).

[9] C. Liu, Z. Dutton, C. H. Behroozi, and L. V. Hau, Nature **409**, 490 (2001).

[10] D. F. Phillips, A. Fleischhauer, A. Mair, R. L. Walsworth, and M. D. Lukin, Phys. Rev. Lett. **86**, 783 (2001).

[11] L. J. Wang, A. Kuzimich, and A. Dogariu, Nature **406**, 277 (2000).

[12] Md. Aminul Islam Talukder, Y. Amagishi, and M. Tomita, Phys. Rev. Lett. **86**, 3546 (2001).

[13] C. G. B. Garret and D. E. McCumber, Phys. Rev. A **1**, 305 (1970).

[14] S. Chu and S. Wong, Phys. Rev. Lett. **48**, 738 (1982).

[15] M. Tanaka, M. Fujiwara, and H. Ikegami, Phys. Rev. A **34**, 4851 (1986).

[16] J. Peatross, S. A. Glasgow, and M. Ware, Phys. Rev. Lett **84**, 2370 (2000).

[17] J. Schwinger, L. L. DeRaad, K. A. Milton, and W. Y. Tsai, *Classical Electrodynamics* (Perseus Book Group, Boston, 1998).

[18] A. I. Talukder, T. Haruta, and M. Tomita, Phys. Rev. Lett. **94**, 223901 (2005).

[19] V. G. Polevoi and S. M. Rytov, Sov. Phys. Usp. **21**, 630 (1978).

[20] O. Kocharovskaya, Y. Rostovtsev, and M. O. Scully, Phys. Rev. Lett. **86**, 628 (2001).

[21] V. M. Agranovich, Y. N. Gartstein, and A. A. Zakhidov, Phys. Rev. B **73**, 045114 (2006).

[22] S. M. Mikki and A. A. Kishk, Prog. Electromagn. Res. B **14**, 149 (2009).

[23] H. Kosaka, T. Kawashima, A. Tomita, M. Notomi, T. Tamamura, T. Sato, and S. Kawakami, Phys. Rev. B **58**, R10096 (1998).

[24] C. Luo, M. Soljacic, and J. D. Joannopoulos, Opt. Lett. **29**, 745 (2004).

[25] N. Malkova, D. A. Scrymgeour, and V. Gopalan, Phys. Rev. B **72**, 045144 (2005).

[26] M. E. Tasgin, Phys. Rev. A **86**, 033833 (2012).